Effects of Natural Aging in Biaxial MEMS Accelerometers

Sergiusz Łuczak, Jakub Wierciak, and Wojciech Credo

***Abstract*—Effects of a fully natural aging of MEMS accelerometers are evaluated with regard to changes in their performance. Two models of commercial dual-axis accelerometers (two pieces of ADXL 202E and 203 by Analog Devices Inc.) with analog outputs were tested over a period of about 10 and 4 years, respectively. A custom computer controlled test rig was used for performing relevant experimental studies, employing the gravitational acceleration as the reference source. A methodology of determining the proposed indicators of aging phenomena is presented and discussed. Changes of the offset voltage and the scale factor were observed and a way of evaluating the overall error due to combined influence of these two parameters is proposed. It was found out that the changes of the output voltage generated by the tested accelerometers were considerable, resulting in respective maximal errors of about 52 mg (2.6%) (ADXL 202E) or 20 mg (1%) (ADXL 203). Simple ways of reducing the effects of aging are proposed.**

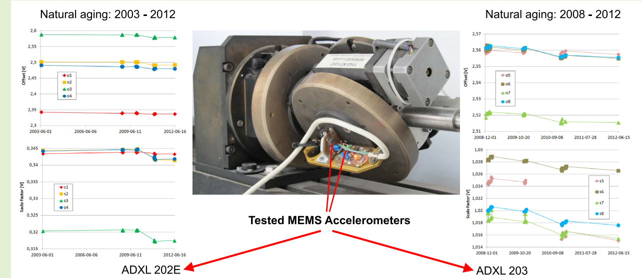

***Index Terms*—Aging, lifetime stability, long-term reliability, MEMS accelerometer, accuracy, tilt.**

I. Introduction

MEMS accelerometers are applied more and more often in many kinds of systems and devices, to directly sense constant or variable acceleration (including vibration) or tilt [1]; owing to appropriate signal processing (integration or differentiation) they also enable determination of velocity and position or jerk and jounce (shock). Due to their small dimensions they are the only solution possible in the case of devices having miniature size, like mobile microrobots [2] and PDAs (Personal Digital Assistant) such as cell phones, tablets, palmtops, photo cameras, smartwatches, or wearable devices like orthotic robots [3]. Over the recent years, even some scuba diving instruments have been equipped with MEMS accelerometers (enabling tilt compensation for the embedded electronic compass [4]), e.g. diving computer Vyper or Cobra by Suunto company [5].

Besides their miniature dimensions, the most advantageous features of MEMS accelerometers are satisfactory metrological parameters, low power consumption, easy integration with electronics, high reliability, high shock-survivability and very low cost, which is of great importance, as it opens new prospects for their application in devices, where a significant increase of the retail price would result in their commercial failure.

In the case of many applications, the lifetime of the final device is usually quite short, and the aging phenomena in the MEMS accelerometer itself may be of marginal importance. However, in the case of some custom devices, like innovative miniature inspection robots, presented e.g. in [6] and [7], their cost may be very high, and thus the time of their operation may be expected to be possibly long. Then, aging of all its components becomes a significant problem, including MEMS sensors, which are usually the only alternative due to the demand for miniature dimensions.

Despite the fact that silicon, the basic material MEMS sensors are made of, is not as prone to aging as e.g. polymers, which quickly demonstrate physical aging, as reported e.g. in [8], [9], nevertheless operational parameters of these low-cost sensors are usually prone to drifting because of premature aging [10].

Thus, in order to obtain possibly high accuracy, including compensation for the aging effects, the output signals generated by MEMS accelerometers can be repeatedly calibrated [11], sometimes in very sophisticated ways, as reported e.g. in [12], [13]. However, in cases when calibration is not repeated within a longer period of time, it would be advantageous to regard the errors due to aging and compensate for them by developing appropriate algorithms.

Manuscript received July 25, 2020; accepted August 10, 2020. Date of publication August 19, 2020; date of current version December 16, 2020. This work was supported by the Scientific Board of the Discipline of Automatics, Electronics and Electrical Engineering, Warsaw University of Technology. The associate editor coordinating the review of this article and approving it for publication was Prof. Sheng-Shian Li. *(Corresponding author: Sergiusz Łuczak.)*

The authors are with the Warsaw University of Technology, Faculty of Mechatronics, 02-525 Warsaw, Poland (e-mail: sergiusz.luczak@pw.edu.pl).

Digital Object Identifier 10.1109/JSEN.2020.3017897

This work is licensed under a Creative Commons Attribution 4.0 License. For more information, see https://creativecommons.org/licenses/by/4.0/

As it is well known, MEMS sensors feature much worse metrological parameters compare to their conventional counterparts. Often, in view of the limited amount of the published data, MEMS devices must be experimentally tested in order to verify their usefulness in certain specific applications. This applies also to the problem of aging, sometimes referred to as lifetime stability.

Natural aging of MEMS sensors is quite an important issue, yet very little data are provided in the related publications. For instance, such companies as STMicroelectronics take into account the effects of aging, designing sophisticated circuits controlling the accelerometers in such a way that some systematic errors, including aging phenomena, are compensated for.

Kajaakari refers to the phenomenon as "drift over lifetime", and proves that some manufacturers of MEMS accelerometers do not regard it at all, whereas others guarantee that the data provided in respective datasheets are valid throughout the whole lifetime of an accelerometer [14].

A survey of the relevant literature provides rather a vague answer to the question of significance of the aging effects in MEMS devices. It is reported that shortcomings of some MEMS devices are related, among other things, to poor knowledge of aging mechanisms [15]. Moreover, quantified results related to aging of monocrystalline silicon are rarely published [16], [17]. Some authors state that results of aging are insignificant, e.g. in [18], [19], whereas others report considerable errors due to aging, exceeding 5%, e.g. in [20]. As far as MEMS accelerometers are concerned, shifts of their bias (offset) were observed in [21], whose maximum value was in range of 0.02 – 7.68 mg in the case of the tested accelerometers embedded into eight different Inertial Measuring Units.

A typical approach while studying aging effects is an accelerated testing, according to e.g. ISO/IEC 60068-2 or 60749-6 standard, where a MEMS device is subjected to high or low temperature, thermal cycling, vibrations (i.e. mechanical fatigue), moisture cycling, etc. [21], [22]. Accelerated testing may be also realized e.g. by harsh electrical loading [23] or subjecting the tested device to some mechanical overloads.

While it is well known that longer life of MEMS is correlated with lower temperatures and lower humidity levels [24], some authors question reliability of such accelerated testing in the case of MEMS, pointing only to the fact that humidity is a major factor accelerating most mechanical and electrical failure modes (thus hermetic packaging is so strategic) [25]. This point of view can be supported by results of a natural aging simulated by storing MEMS accelerometers at higher temperatures, when only small changes in their performance were reported in [26], [27].

Moreover, some research teams claim that it is crucial to distinguish between short-term and long-term degradation mechanisms in order to avoid a wrong lifetime prediction [28].

In light of the above, it may be stated that at this stage, the most reliable method of evaluating the considered effects is natural aging. For example, in [29] the authors tested over a period of 18 months five different inertial measuring units (IMU) containing MEMS accelerometers. As reported, the observed changes were insignificant. However, many factors were involved here, as not only the accelerometers had been subjected to aging but the IMUs as a whole (including the circuits processing the output signals generated by the accelerometers). Besides, it is hard to state whether the tested IMUs had some embedded algorithms compensating for the aging effects of their components (including the accelerometers).

The aging phenomena can be related to particular elements of MEMS accelerometer:

- mechanical components (mainly the elastic suspension of the seismic mass),
- electric components (mainly capacitive or piezoelectric transducers converting deflection of the elastic suspension of the seismic mass into a change of some electric quantity),
- electronic circuits (integrated with the mechanical structure – surface micro-machining, or a separate chip – bulk micro-machining),
- external electronic components setting operational parameters of the accelerometer, especially the constant-voltage regulator.

From a cognitive point of view, each element could be studied separately with regard to the effects of its aging. Unfortunately, the results presented in this article do not make it possible to distinguish between particular elements, and concern the entire accelerometer together with the basic electronic circuit (external capacitors and resistors, constant-voltage regulator) as a whole. Such approach has a general character, yet is more convenient from the point of view of a practical application. It evaluates performance of the accelerometer as a whole, what is more interesting for a potential user of such sensor.

Due to a lower quality of the employed material, it can be expected that surface micro-machined MEMS devices (based on poly-crystalline silicon) are more prone to aging effects than their counterparts fabricated by bulk micro-machining (based on mono-crystalline silicon). So, it was decided to test accelerometers manufactured by surface machining, since a chance for observing noticeable changes seemed to be more probable in this case.

Throughout the whole time of testing (2003-2012), the tested accelerometers have been stored in laboratory rooms, where the ambient temperature was in the range not exceeding 15-40°C (however during calibration the range was 20-30°C; nevertheless, the chips themselves may have been subjected to higher temperatures due to internal ohmic losses; their supply voltage was 5V).

II. Experimental Studies

One of the applications of accelerometers are tilt measurements [1]. Since in this case the measurand is the gravitational acceleration, being one of the most stable and accurate external reference sources available [30]–[32], it is very convenient to employ it in experimental studies, and thus it is often used by various research teams, e.g. in [33]. In the case of low-g accelerometers it provides satisfactory variation range of the reference acceleration, what sometimes is a problem while

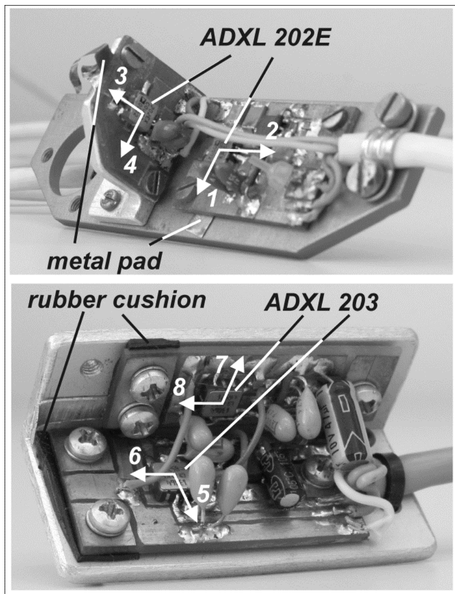

Fig. 1. The tested accelerometers.

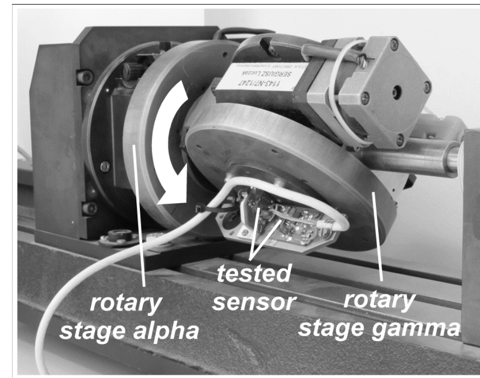

Fig. 2. Calibration by applying pitch angle.

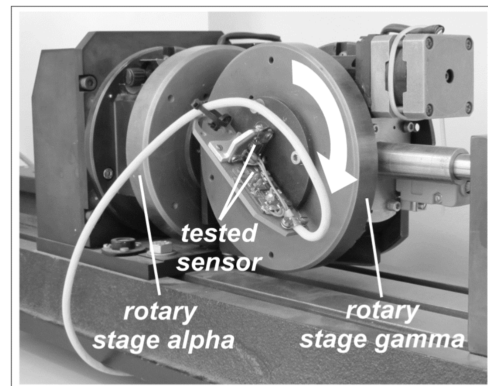

Fig. 3. Calibration by applying roll angle.

generating acceleration by means of a standard equipment, like e.g. a nano-positioning stage used in experimental studies reported in [34], [35].

In order to evaluate the considered effects of aging to be observed in MEMS accelerometers, it was decided to repeat many times (90 altogether) a calibration procedure over a long-term period. The calibration consisted in changing position of the tested accelerometer with respect to the gravity vector and then recording its output signals. The position was changed within only one of two vertical planes at a time. As the accelerometers were arranged in such a way as to create a triaxial acceleration sensor (corresponding to a dual-axis tilt sensor), the plane was either pitch plane or vertical roll plane (with no pitch involved – see Fig. 2, 3). Two kinds of dual-axis MEMS accelerometers by Analog Devices Inc. were tested: ADXL 202E (manufactured no later than 2002) and ADXL 203 (manufactured no later than 2005). As the manufacturer declares, ADXL 203 is an improved version of 202E, so both accelerometers were similar. Besides, as the manufacturer states, ADXL 203 features low noise and good thermal stability, and thus it has been sold by the manufacturer hitherto (i.e. for over 15 years). The accelerometers (two pieces of each kind) are presented in Fig. 1 (axes 1 – 8 labeled on the figure are the sensitive axes of the accelerometers, referred to later in the text).

In the experiments, two pieces of each dual-axis accelerometer were used at the same time. Thus, components of the gravitational acceleration were measured in x, y, z axis, yet in the case of ADXL 202E there were two x axes, whereas two y axes for ADXL 203. Referring to the initial position of the accelerometers while fixed in the test rig, axes *1*, *4*, *5* correspond to x axis, axes *2*, *6*, *8* to y axis, and axes *3*, *7* to z axis.

The calibration made it possible to determine parameters of the analog output signals of the accelerometers. The signals can be represented by the following formulas:

$$U_x = o_x + s_x \sin(\alpha + p_x) \quad (1)$$

$$U_y = o_y + s_y \sin(\gamma + p_y) \quad (2)$$

$$U_z = o_z + s_z \cos(\alpha + p_{z\alpha}) \quad (3)$$

$$U_z = o_z + s_z \cos(\gamma + p_{z\gamma}) \quad (4)$$

where: U_x, U_y, U_z – output voltage assigned to x, y or z axis [V]; o_x, o_y, o_z – offset (bias) of the output voltage assigned to U_x, U_y or U_z [V]; s_x, s_y, s_z – scale factor (sensitivity, gain) of the output voltage assigned to U_x, U_y or U_z [V]; p_x, p_y, $p_{z\alpha}$, $p_{z\gamma}$ – geometrical phase shift of the output voltage assigned to U_x, U_y or U_z [deg]; α – pitch applied by means of the test rig (rotary stage alpha – see Fig. 2) [deg]; γ – roll applied by means of the test rig (rotary stage gamma – see Fig. 3) [deg].

The calibration process was realized by means of a special test rig, whose main elements were two rotary stages (applying pitch and roll angles respectively) controlled by a computer with a data acquisition module (Advantech PCL 818L/PCI 1716) installed for reading the analog output voltages of the accelerometers. The mechanical part of the test rig is presented in Fig. 2, 3. The whole test rig has been minutely described in [36]. It is characterized by the following features:

- measurements of the analog output voltages of the tested accelerometers realized by means of the analog/digital module with uncertainty of 0.0016 V (at the confidence level $p = 99\%$),

- application of angular position of the tested accelerometer with precision of at least 1.2 minute arc (±0.02°) over the full range of pitch and roll.

The test rig makes it possible to perform only static tests. It is built of similar components like those used in the experimental setup reported e.g. in [37], yet its geometrical structure is more developed and precise. In the case when other ultimate effects of aging, like changes of the dynamic properties of accelerometers would be searched for, e.g. phase-shift and scale factor attenuation (accelerometer frequency response) while increasing the frequency, a more sophisticated test rig must be used, e.g. similar to the one presented in [38].

Nevertheless, despite limitations of the employed test rig pertaining to dynamic operation, it features a high kinematic precision owing to accurate integration of the rotary stages into one mechanical structure, in order to avoid various positioning errors minutely discussed e.g. in [39].

III. Results

Detailed description of the employed methodology of performing the experimental studies using the test rig, including the alignment procedure [40], has been presented in [41]. In short, the reported results were obtained as follows.

The computer activated a respective rotary stage (the rotation axis of the active stage was always horizontal during the tests), set its desired position, and then recorded series of the corresponding output voltages of the tested accelerometers. While recording the output signal/signals assigned to x axis, the rotary stage alpha was powered (pitch angle) – Fig. 2, whereas for obtaining the output signal/signals assigned to y axis the rotary stage gamma was put in motion (roll angle) – Fig. 3. The output signal assigned to z axis was recorded in both cases.

Each test consisted in rotating the accelerometers over the full range (360°) of pitch or roll, respectively. In most of the cases, the angular positions were changed with a step of 1° (in some cases 5° due to lack of time – see explanation in Sec. Acknowledgements). At each angular position, when the rotary stage had already reached the desired position and was immobile, the output voltages were sampled 30 times and their values recorded in the computer memory. So, each calibration consisted of 10,800 records (or 2,160 at 5° steps).

In the case of applying the roll angle, each calibration procedure was preceded by calibrating the accelerometers with respect to pitch, in order to precisely find the zero-pitch angle and only then apply pure roll angle in the next step.

In order to determine parameters $o_{x..z}$, $s_{x..z}$, $p_{x..z}$ of Eq. (1)-(4), the recorded data were processed by means of statistical software (Statgraphics), employing a nonlinear regression model consistent with Eq. (1)-(4).

Some research teams, e.g. in [34], [35], proposed another approach, where only extreme indications of the accelerometer are used (when each sensitive axis is oriented upwards and then downwards) to determine parameters $o_{x..z}$ and $s_{x..z}$ – i.e. the offset (also referred to as "zero-measurand-output" [38]) and the scale factor (sometimes improperly called "sensitivity" or "gain"). Yet, as our study reported in [40] proves,

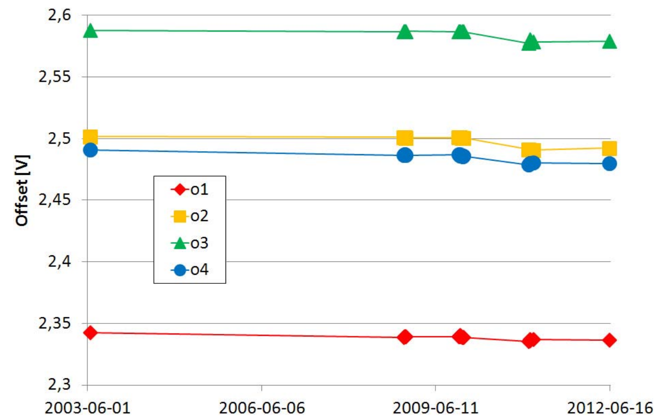

Fig. 4. Changes of the offset of ADXL 202E over time.

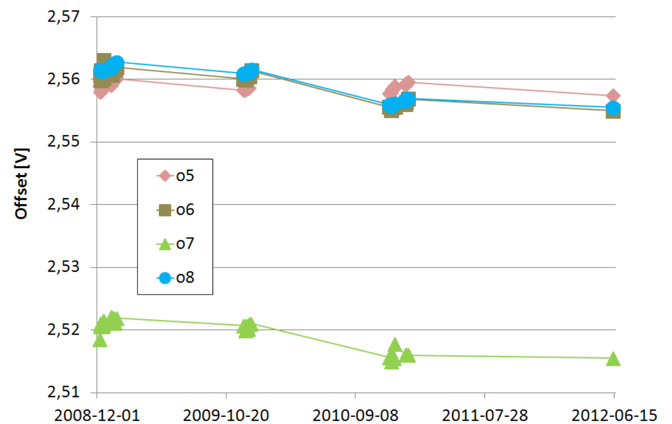

Fig. 5. Changes of the offset of ADXL 203 over time.

the parameters determined according to both methods reveal no significant difference in their values. However, while determining only extreme values of the output voltage of particular sensitive axis, the existing misalignments cannot be detected [41].

Graphs presented in Sec. A and B were created on the basis of the same set of data. It was accepted that subscripts of the offset $o_{x..z}$ and the scale factor $s_{x..z}$ are consistent with the labels of the sensitivity axes of the accelerometers introduced in Fig. 1. Due to lack of time (see Sec. Acknowledgements), while testing the accelerometers not all the output signals of the accelerometers were tested in each study. The presented data consist of 32 calibration procedures for ADXL 202E and 58 for ADXL 203 (this can be expressed as about 96 or 174 hrs of operation, respectively). Due to considerable differences in average values of parameters related to particular axes, the scale on the vertical axis is different for each graph (Fig. 4-7).

A. Offset

Changes of the offsets of the two accelerometers over the whole time of testing are illustrated in Fig. 4 and Fig. 5.

It is interesting that within the first 6.5 years no considerable changes of the offsets $o_1 - o_4$ were detected (the same applies to the scale factors – Fig. 6), whereas the offsets $o_5 - o_8$

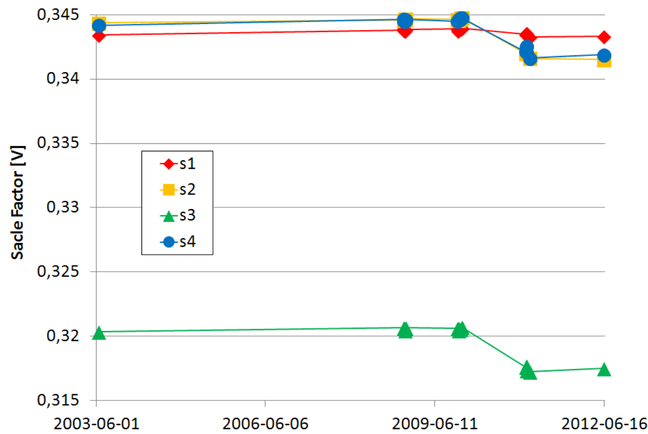

Fig. 6. Changes of the scale factor of ADXL 202E over time.

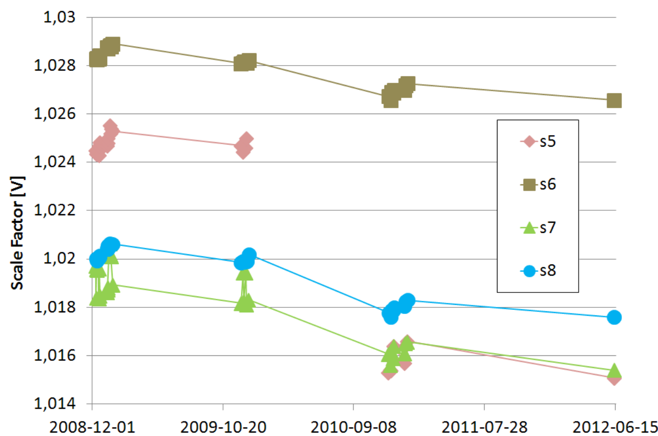

Fig. 7. Changes of the scale factor of ADXL 203 over time.

had been changing from the very beginning. It proves the aforementioned suggestion to distinguish between short-term and long-term degradation [28] to be right.

All the courses have a similar character. Differences in the average level of the offsets result from individual properties of the accelerometer.

Smaller amount of data related to o_5 and s_5 (Fig. 5, 7) results from a limited time for performing a corresponding test (see Sec. Acknowledgements).

B. Scale Factor

Changes of the scale factor of the two accelerometers over the whole time of testing are illustrated in Fig. 6 and Fig. 7.

The scale factor is usually expressed in volts per g [V/g], e.g. in [29], [35]. Yet, for the sake of simplicity and clarity of the presented formulas, it was assumed that this parameter was expressed in Volts.

Thus, in order to determine acceleration a [m/s^2] measured by an analog MEMS accelerometer calibrated as aforementioned, the following formula must be used:

$$a_{x..z} = m_{x..z} \cdot g \tag{5}$$

where: g – gravitational acceleration (about 9.78 – 9.83 [m/s^2]; 9.81 in Warsaw, Poland); $m_{x..z}$ – relative acceleration

TABLE I
MAXIMAL CHANGES OF THE OFFSET AND THE SCALE FACTOR (ADXL 202E)

Accelerometer No.	Parameter	Original Value [V]	Absolute Change [V]	Relative Change (%)
#1	o_1	2.3426	0.0073	0.31
#1	s_1	0.3434	0.0006	0.16
#1	o_2	2.5017	0.0110	0.44
#1	s_2	0.3444	0.0029	0.83
#2	o_3	2.5879	0.0103	0.40
#2	s_3	0.3204	0.0031	0.97
#2	o_4	2.4909	0.0122	0.49
#2	s_4	0.3442	0.0025	0.74

TABLE II
MAXIMAL CHANGES OF THE OFFSET AND THE SCALE FACTOR (ADXL 203)

Acceleromete r No.	Paramete r	Original Value [V]	Absolute Change [V]	Relative Change (%)
#3	o_5	2.5589	0.0015	0.06
#3	s_5	1.0245	0.0094	0.92
#3	o_6	2.5607	0.0058	0.22
#3	s_6	1.0283	0.0017	0.17
#4	o_7	2.5185	0.0035	0.14
#4	s_7	1.0197	0.0043	0.42
#4	o_8	2.5616	0.0060	0.24
#4	s_8	1.0200	0.0024	0.24

in x, y, z axis (respectively) in terms of a multiple of g, computed as (disregarding the phase shifts, which can be physically eliminated):

$$m_{x..z} = \frac{U_{x..z} - o_{x..z}}{s_{x..z}}. \tag{6}$$

Courses s_2 and s_4 corresponding to the scale factors of ADXL 202E are almost the same (see Fig. 4). Except for the scale factor s_1, the other courses have a similar character. Yet, the existing differences prove that the observed changes originated rather in the tested accelerometer, and not in the other components involved (constant-voltage regulator, measurement circuit, etc.).

As far as ADXL 203 is concerned, rapid changes of s_7 (dated about 2008 and 2009) and a large decrease of s_5 (dated about 2009-2010) were caused most probably by a faulty soldered joint of the accelerometer with the PCB (see the explanation provided later in the text).

Maximal absolute and relative (with respect to the value determined most early) changes of the offset and the scale factor observed over the whole time of the experiments are presented in Table I and Table II.

In Table I, the absolute changes of the offset are of 0.0073 – 0.0122 V, whereas the absolute changes related to the scale factor vary over a smaller range of 0.0006 – 0.0031 V. However, since the offset is of a larger value than the scale factor, the relative changes are 0.31% – 0.49% and 0.16% – 0.97%, respectively.

While determining the considered parameters for each calibration procedure, values of the respective adjusted R-squared coefficient (determination coefficient) were in the range of 99.9982% – 99.9994% (in the case of most of the procedures, when the angular step was of 1°), what confirms that the obtained data are reliable.

In Table II we observe smaller variations compare to Table I. The absolute changes of the offset are of 0.0015 – 0.0060 V (0.06% – 0.24%), whereas the absolute changes related to the scale factor vary over a wider range of 0.017 – 0.0094 V (0.17% – 0.92%).

In the case of determining the considered parameters for each calibration procedure related to axes #6, #7 and #8, values of the respective adjusted R-squared coefficient were in the range of 99.9995% – 99.9998%. However, significantly lower value of the adjusted R-squared coefficient (99.9850%) was observed for axis #5. It resulted from the fact that the electronic circuit of the sensitive axis #5 of ADXL 203 had not operated properly. Yet for didactic purposes the failure was not eliminated. The related output signal was very noisy (with the noise level about 10 times higher compare to the other sensitive axes), probably due to some defective soldered joint. This resulted also in an untypical proportion of changes presented in Table II.

C. Uncertainty of the Determined Acceleration

In the case of determining tilt angles $m_{x..z} \in \langle -1, 1\rangle$, whereas in the case of using the whole measurement range of the tested accelerometers ($\pm 2g$), $m_{x..z} \in \langle -2, 2\rangle$.

Having determined the relative acceleration $\Delta m_{x..z}$ by means of Eq. (6), its absolute maximal error with respect to the constituent variables can be computed as follows [43],

$$\Delta m_{x..z} = c_o \Delta o_{x..z} + c_s \Delta s_{x..z} + c_U \Delta U_{x..z}, \tag{7}$$

where c_o, c_s, c_U are sensitivity coefficients [44], related to the offset, the scale factor and the output voltage, respectively, which can be evaluated as follows [44]:

$$c_o = \left|\frac{\partial m_{x..z}}{\partial o_{x..z}}\right| = \frac{1}{s_{x..z}}, \tag{8}$$

$$c_s = \left|\frac{\partial m_{x..z}}{\partial s_{x..z}}\right| = \frac{1}{s_{x..z}} \cdot \frac{|U_{x..z} - o_{x..z}|}{s_{x..z}} = c_o \frac{|U_{x..z} - o_{x..z}|}{s_{x..z}}, \tag{9}$$

$$c_U = \left|\frac{\partial m_{x..z}}{\partial U_{x..z}}\right| = \frac{1}{s_{x..z}} = c_o. \tag{10}$$

As far as evaluation of the accelerometer performance over time is concerned, the most interesting case is when Eq. (7) takes on the maximal value. Let us disregard at this point the influence of variations of the output voltage expressed by Eq. (10) as not related directly to aging phenomena. So, comparing the sensitivity coefficients c, see Eq. (8) - (9), we see that in order to find relation between c_o and c_s, the following inequalities must be analyzed:

$$|U_{x..z} - o_{x..z}| \leq s_{x..z}, \tag{11}$$

TABLE III
MAXIMAL ERRORS OF THE MEASURED ACCELERATION (ADXL 202E, 203)

Sensor	Acceleration	$c_o\Delta o_i$	$c_s\Delta s_i$	ΔM_i	δM_i (%)	ΔA_i [mg]
202E	m_1 (m_x)	*0.0212*	0.0033	0.0245	1.2	25
202E	m_2 (m_y)	*0.0319*	0.0166	0.0485	2.4	49
202E	m_3 (m_z)	*0.0321*	0.0195	0.0516	2.6	**52**
202E	m_4 (m_x)	*0.0355*	0.0148	0.0503	2.5	50
203	m_5 (m_x)	*0.0015*	0.0180	0.0198	1	**20**
203	m_6 (m_y)	*0.0056*	0.0033	0.0089	0.4	9
203	m_7 (m_z)	*0.0034*	0.0085	0.0119	0.6	12
203	m_8 (m_y)	*0.0059*	0.0048	0.0107	0.5	11

$i=x, y, z$; 1 mg = 0.00978 – 0.00983 [m/s^2]

or

$$|U_{x..z} - o_{x..z}| \geq s_{x..z}. \tag{12}$$

If Eq. (11) is true, then $c_o \geq c_s$, and if Eq. (12) is true, then $c_s \geq c_o$. If the scale factor were determined as corresponding to the full measurement range of the accelerometer, Eq. (11) would be always true. However, in our case the scale factor corresponds to half of the measurement range, so for accelerations $|a_{x..z}| \leq 1g$ (e.g. tilt measurements) $c_o \geq c_s$, otherwise $c_o \leq c_s$.

Effects of the maximal changes of the offset and the scale factor on the relative acceleration $m_{x..z}$ are shown in Table III. When calculating maximal absolute acceleration errors $\Delta M_{x..z}$, and maximal relative errors $\delta M_{x..z}$ (referred to the measurement range) according to Eq. (13) and (14), the worst case was assumed, which corresponds to the full measurement range (when $m_{x..z} = \pm 2g$ and $c_o \leq c_s$.), i.e. to a situation when the maximal value of $U_{x..z}$ is measured, so:

$$\Delta M_{x..z} = \frac{\Delta o_{x..z}}{s_{x..z}} + \frac{2\Delta s_{x..z}}{s_{x..z}}, \tag{13}$$

so the analyzed influence of changes of the scale factor was twice as much as of the offset.

Combining Eq. (7)-(9) and (13), the relative maximal error $\delta M_{x..z}$ of determining the acceleration corresponding to the full measurement range can be evaluated as [46]:

$$\delta M_{x..z} = \frac{\Delta o_{x..z} + 2\Delta s_{x..z}}{2 s_{x..z}}. \tag{14}$$

Besides the values of maximal errors ΔM_i and δM_i of the relative acceleration m_i, the corresponding values of the absolute acceleration ΔA_i are given in Table III.

Significant differences in the total error exist not only between particular accelerometers, but between their sensitive axes as well, what implies a random character of the observed aging phenomena.

As the data in Table III confirm, it is the change of the offset that influences the error of the relative acceleration $m_{x..z}$ the most (see Eq. (7)), with two exceptions: m_5 and m_7.

IV. Discussion

Since the studied aging effects involve changes related to many different components, it is hard to explain the character of courses presented in Fig. 4 – 7. However, individual character of courses and values related to particular axes suggest that most of the aging effects took place in the accelerometer itself, since long-term changes in other components of the measurement circuit would have resulted in a similar character of variations related to all the sensitive axes.

Looking at the presented courses, it can be clearly observed that the changes of the offset and the scale factor are significantly bigger over a longer period compare to small variations within short periods of time.

The observed changes of the offset are affecting the maximal error few times more than the changes of the scale factor, except for two cases (m_5 and m_7 in Table III – in both cases the blame is to be put on the defective soldered joints).

They are not of a linear or even systematic character (differences between particular sensitive axes occurred), what makes it difficult to create exact models of aging in order to compensate for the relevant errors. Nonetheless, some less accurate models of the studied phenomena can be surely introduced.

Values of the maximal errors are slightly over-estimated in the sense that they were computed assuming maximal changes of both the offset and the scale factor, what must not be necessarily the case; however courses presented in Fig. 4-7 illustrate that rather both of these parameters changed in a similar way.

There are few other factors that most probably will considerably intensify the aging effects. These are: mechanical overloads (including high-g shocks) of the accelerometer both while operated as well as stored (the tested accelerometers were not overloaded within their whole life), scatter of various operational parameters within the production batch (in the case of the tested accelerometers it is a considerable factor, as reported in the relevant datasheets [31], [32]), material fatigue of mechanical members of the accelerometer. So, it is rather certain that the values of errors related to aging phenomena will be in many cases much bigger than the reported.

A. Thermal Drifts

An important issue that must be taken into account are thermal drifts of the offset and the scale factor. Even though most of the experiments were conducted at temperatures of 24-27°C, there were cases when the temperature was in the range of 20-30°C. Analyzing the related thermal coefficients specified in [31], [32], it can be stated that thermal drifts of the scale factor can be neglected, whereas maximal values of the thermal drifts of the offset are relatively large compare to the observed changes (in an extreme case up to 40%).

However, the datasheets [31], [32] reveal a considerable scatter of possible values of the thermal coefficients for a specific piece of accelerometer. Thus, we decided to experimentally determine the thermal drift of the offset voltage of each of the eight sensitive axes within temperature range of 19-31°C (202E) and 19-35°C (203).

Except for the offset o_5 (associated with the defective soldered joint), average value of the thermal drifts did not exceed 30% of the changes attributed to aging effects evaluated in Tab. I and II; the highest percentage value of the thermal drift equal to 64% was observed only in the case of offset o_1.

Moreover, only small variations of the offset and the scale factor can be observed over short spans of time (when different temperatures occurred with no coexisting aging effects). Thus, we assume that the existing thermal drifts had even smaller impact than it results from the determined values. The thermal drifts are probably the main reason for small short-term variations of the offset and the scale factor observed in Fig. 4-7 (more clearly in the case ADXL 203, since the voltage values over the y-axis are in smaller range).

B. Increasing Accuracy of the Measurements

Analyzing Eq. (7) and (9), it can be stated that a better accuracy of the accelerometer can be obtained when we use values of its indications corresponding to accelerations of small magnitude. In the case of measuring tilt it takes place when $U_{x..z} \approx o_{x..z}$, i.e. for $\alpha \approx 0°$ or $\gamma \approx 0°$. So, this idea resolves itself into using only a fragment of the measuring range or assigning a higher priority to this fragment. While comparing measurements of acceleration of about $0g$ and $\pm 2g$, in the case of ADXL 202E accelerometers the evaluated errors due to aging would decrease then from 52 mg (2.6%) down to 36 mg (1.8%), whereas for ADXL 203 from 20 mg (1%) down to 6 mg (0.3%). So, a considerable increase of accuracy can be achieved.

If acceleration with amplitude of about $\pm 1g$ is measured, the sensitive axis of the accelerometer should be oriented vertically, if possible, so that the difference between the gravity acceleration and the measured acceleration would be small. If the amplitude were lower than $\pm 1g$, the accelerometer should be tilted in such a way, as to obtain a low value of the resultant acceleration. However, cross-axis sensitivity of the accelerometer should be taken into consideration in this case.

C. Tilt Measurements

As far as tilt measurements are concerned, where only half of the measurement range is used ($\pm 1g$), thus Eq. (14) must be adjusted to this range, the maximal observed changes of the measured acceleration are higher, i.e. 86 mg (4.3%) for ADXL 202E or 22 mg (1.1%) for ADXL 203, what would correspond to angular error of about 2.5° or 0.6°, respectively.

D. Mounting of the Accelerometer

It is well known that mounting of the accelerometer-chips should be considered an important issue, e.g. additional gluing of the chip to the PCB (strengthening the soldered joints) may prevent from limitation of the bandwidth in the case when the accelerometers operate under dynamic conditions. A careful attention must be paid to the mounting of the whole PCB

with the accelerometer-chip, if related effects of aging are to be limited. So, the PCB should be firmly and durably fixed to the housing, using appropriate materials – some materials, like rubber (see Fig. 1) or polymers, may considerably change their properties and dimensions over time.

E. Accuracy of the A/D Modules

Error of measuring the analog output voltages of the tested accelerometer realized by means of the applied analog/digital modules was no higher than 0.0016 V [36]. Then its influence on the determined acceleration can be evaluated using Eq. (10). So, in this case it would be of about 0.005 V for ADXL 202E and 0.0016 V for ADXL 203, i.e. 0.5% and 0.16%, respectively. Comparing it to the component errors due to aging, it can be stated that this influence has an acceptable magnitude in this analysis.

If the AXDL 203 accelerometers were as old as ADXL 202E, the maximum relative change (multiplied by about 2.7 – assuming a linear character of aging effects) would be approximately the same, i.e. 2.7%.

Within the testing period, in 2009, a PCL 818L 12-bit analog/digital acquisition module was replaced with a PCI 1716 16-bit module, which features a bit better accuracy. No significant difference in the obtained results was observed, what results also from the fact that both modules featured similar accuracy according to the relevant datasheets. Besides, it proves that aging effects associated with the modules were also insignificant.

As can be observed, the tested pieces of the accelerometers reveal rather no individual character of the observed changes (except for changes of scale factor s_1 in Fig. 6 and s_7 in Fig. 7, the later resulting from a faulty operation of the accelerometer).

The graphs illustrated in Fig. 4 – 7 indicate a trend suggesting further, even more intensive, changes over the time. In order to verify this presumption, it is planned to repeat the reported studies in few years time.

The range of the ambient temperature of (15-40°C), under which the accelerometers were stored, was quite narrow, what may not be the case in many applications, where the main device operates or is stored under more severe conditions. Especially higher temperatures may be critical, as they speed up the process of aging of MEMS devices [26], [27]. So, generally, the evaluated values of errors due to aging will be rather of higher values.

V. Conclusion

The presented study was not an attempt to carefully investigate particular aging mechanisms but rather to evaluate the overall effects of aging, providing practical information, useful both for the scientific community as well as engineers.

A considerable decrease of accuracy due to natural aging phenomena was determined in terms of changes of the offset and the scale factor. Additionally, it was discovered that the mounting technique is also important (attaching the MEMS accelerometer to the PCB and fixing the PCB to the housing - see Fig. 1).

The evaluated maximal errors due to aging of the tested accelerometers, the electronic components on the accelerometer PCBs (especially the constant-voltage regulators) are considerable, thus cannot be overlooked in the case of applying MEMS accelerometers where accuracy of about 1% is expected to last over a longer period of time (few years or more).

An example of such critical application may be modern enhanced motorcycle ABS systems employing relatively precise tilt measurements by means of MEMS inertial sensors [45], where human life and safety is at stake, and the vehicle may be in use for decades.

Concluding, even though the observed effects are quite considerable, in the case of using similar MEMS accelerometers under more harsh conditions (frequent operation – resulting in material fatigue, mechanical overloads/shocks, wide range of changes of the ambient temperature) even bigger changes of their operational parameters should be taken into account.

On the other hand, if MEMS accelerometers have been used under conditions similar to the reported (storing period of 10/4 years, total operation time of about 100/200 hrs, ambient temperature in the range 15 – 40°C) the presented numerical values are fully relevant.

The maximal values of errors obtained for both types of accelerometers are much lower than the maximal value of 5% [20] found in the relevant publications. However, compare to the aging effects related to similar, yet triaxial, accelerometers (ADXL 330, ADXL 327), which we have reported recently, error values listed in Table III (1.2 – 2.6% for ADXL 202E; 0.4 – 1% for ADXL 203) are similar to their triaxial counterparts (0.4 – 0.8%) [46], especially with regard to ADXL 203.

A proposal of reduction of the considered errors (based on setting an appropriate orientation of the accelerometer) from 52 mg (2.6%) to 36 mg (1.8%) or 20 mg (1%) to 6 mg (0.3%), for ADXL 202E and 203 respectively, was suggested in Sub-section IV.B.

Another way of reducing the errors due to aging is to apply systems that can be calibrated while operated (including corrections for the misalignment angles), like e.g. 3DM-GX3-25 by MicroStrain Inc. Then, the related errors can be compensated for to some extent, and thus the described effects reported in the article considerably minimized.

However, assuming such repeatable calibration, it must not be forgotten that alignment precision, being a crucial issue pertaining to application of MEMS accelerometers, especially with respect to their calibration accuracy [47], may be also a subject to aging processes. Alignment precision is a matter of great importance in the case of determining tilt angles [48], especially while striving for high accuracy of the measurements [49], as proved e.g. by result of experimental studies reported in [50].

As the magnitudes of the reported aging effects were surprisingly large, it is foreseen to continue similar studies of other MEMS accelerometers being operated in the laboratory.

Acknowledgment

The authors would like to express their gratitude to the students of the Faculty of Mechatronics, specializing in Micromechanics, for their diligent realization of the experimental works during a laboratory class "Studies of tilt sensors" within academic years 2008/09 – 2012/13. The obtained results constitute an essential part of the data used for processing the final results presented in the article.

References

[1] J. S. Wilson, *Sensor Technology Handbook*. Burlington, MA, USA: Newnes, 2005, pp. 398–399.

[2] S. Fatikow and U. Rembold, *Microsystem Technology and Microrobotics*. Berlin, Germany: Springer-Verlag, 1997, p. 226.

[3] J. Wierciak, K. Bagiński, D. Jasińska-Choromańska, and T. Strojnowski, "Orthotic robot as a self optimizing system," in *Recent Technological and Scientific Advances*, T. Brezina and R. Jabloński, Eds. Cham, Switzerland: Springer, 2014, pp. 607–614.

[4] M. Reinstein, "Evaluation of fine alignment algorithm for inertial navigation," *Przegld Elektrotechniczny*, vol. 87, no. 7, pp. 255–258, 2011.

[5] S. Łuczak, R. Grepl, and M. Bodnicki, "Selection of MEMS accelerometers for tilt measurements," *J. Sensors*, vol. 2017, pp. 1–13, 2017. Article ID 9796146

[6] M. Bodnicki and D. Kamiński, "In-pipe microrobot driven by SMA elements," in *Recent Technological and Scientific Advances*, T. Brezina and R. Jabloñski, Eds. Cham, Switzerland: Springer, 2014, pp. 527–533.

[7] M. Bodnicki and M. Sęklewski, "Design of small-outline robot—Simulator of gait of an amphibian," in *Recent Technological and Scientific Advances*, R. Jabłoński, M. Turkowski R. Szewczyk, Eds. Berlin, Germany: Springer-Verlag, 2007, pp. 77–81.

[8] G. M. A. Alves, S. B. Goswami, R. D. Mansano, and A. Boisen, "Temperature modulated nanomechanical thermal analysis," *IEEE Sensors J.*, vol. 18, no. 10, pp. 4001–4007, May 2018.

[9] W. S. de Araujo Rocha, J. C. Grilo Rodrigues, A. A. A. Exposito de Queiroz, and A. A. A. de Queiroz, "Curcumin nanocrystals as photodynamical sensor monitoring ultraviolet accelerated aging of HDPE," *IEEE Sensors J.*, vol. 20, no. 1, pp. 155–161, Jan. 2020.

[10] F. Delaine, B. Lebental, and H. Rivano, "*In situ* calibration algorithms for environmental sensor networks: A review," *IEEE Sensors J.*, vol. 19, no. 15, pp. 5968–5978, Aug. 2019.

[11] S. Nadig and A. Lal, "*In-situ* calibration of MEMS inertial sensors for long-term reliability," in *Proc. IEEE Int. Rel. Phys. Symp. (IRPS)*, Burlingame, CA, USA, Mar. 2018, pp. 1–8.

[12] T. Dar, K. Suryanarayanan, and A. Geisberger, "No physical stimulus testing and calibration for MEMS accelerometer," *J. Microelectromech. Syst.*, vol. 23, no. 4, pp. 811–818, Aug. 2014.

[13] I. Frosio, F. Pedersini, and N. A. Borghese, "Autocalibration of triaxial MEMS accelerometers with automatic sensor model selection," *IEEE Sensors J.*, vol. 12, no. 6, pp. 2100–2108, Jun. 2012.

[14] V. Kaajakari, *Practical MEMS*. Las Vegas, NV, USA: Small Gear, 2009, p. 174.

[15] A. Tazzoli, G. Cellere, E. Autizi, V. Peretti, A. Paccagnella, and G. Meneghesso, "Radiation sensitivity of ohmic RF-MEMS switches for spatial applications," in *Proc. IEEE 22nd Int. Conf. Micro Electro Mech. Syst.*, Jan. 2009, pp. 634–637.

[16] A. Neels, A. Dommann, A. Schifferle, O. Papes, and E. Mazza, "Reliability and failure in single crystal silicon MEMS devices," *Microelectron. Rel.*, vol. 48, nos. 8–9, pp. 1245–1247, Aug. 2008.

[17] A. Neels, G. Bourban, H. Shea, A. Schifferle, E. Mazza, and A. Dommann, "Aging of MEMS—Correlation of mechanical and structural properties," *Procedia Chem.*, vol. 1, no. 1, pp. 820–823, Sep. 2009.

[18] A. Ya'akobovitz and S. Krylov, "Toward sensitivity enhancement of MEMS accelerometers using mechanical amplification mechanism," *IEEE Sensors J.*, vol. 10, no. 8, pp. 1311–1319, Aug. 2010.

[19] Y. Yang *et al.*, "Nonlinearity of degenerately doped bulk-mode silicon MEMS resonators," *J. Microelectromech. Syst.*, vol. 25, no. 5, pp. 859–869, Oct. 2016.

[20] X. Xiong, Y.-L. Wu, and W.-B. Jone, "Material fatigue and reliability of MEMS accelerometers," in *Proc. IEEE Int. Symp. Defect Fault Tolerance VLSI Syst.*, Boston, MA, USA, Oct. 2008, pp. 314–322.

[21] A. S. Önen and Y. Günhan, "Accelerated aging test for MEMS inertial measurement units using temperature cycling," in *Proc. IEEE/ION Position, Location Navigat. Symp. (PLANS)*, Monterey, CA, USA, Apr. 2018, pp. 546–551.

[22] J. Dhennin, D. Lellouchi, and F. Pressecq, "How to evaluate the reliability of MEMS devices without standards," in *Proc. Symp. Design, Test, Integr. Packag. MEMS/MOEMS (DTIP)*, Apr. 2015, pp. 1–3.

[23] K. Krupa, C. Gorecki, R. Jóźwicki, M. Józwik, and A. Andrei, "Interferometric study of reliability of microcantilevers driven by AlN sandwiched between two metal layers," *Sens. Actuators A, Phys.*, vol. 171, no. 2, pp. 306–316, Nov. 2011.

[24] D. M. Tanner *et al.*, "Accelerating aging failures in MEMS devices," in *Proc. IEEE Int. Rel. Phys. Symp.*, Apr. 2005, pp. 317–324.

[25] H. R. Shea, "Reliability of MEMS for space applications," *Proc. SPIE*, vol. 6111, Jan. 2006, Art. no. 61110A.

[26] S. Habibi, S. J. Cooper, J.-M. Stauffer, and B. Dutoit, "Gun hard inertial measurement unit based on MEMS capacitive accelerometer and rate sensor," in *Proc. IEEE/ION Position, Location Navigat. Symp.*, 2008, pp. 232–237.

[27] F. Schneider, T. Fellner, J. Wilde, and U. Wallrabe, "Mechanical properties of silicones for MEMS," *J. Micromech. Microeng.*, vol. 18, no. 6, Jun. 2008, Art. no. 065008.

[28] M. Barbato, A. Cester, and G. Meneghesso, "Viscoelasticity recovery mechanism in radio frequency microelectromechanical switches," *IEEE Trans. Electron Devices*, vol. 63, no. 9, pp. 3620–3626, Sep. 2016.

[29] M. Šipoš, P. Pačes, J. Roháč, and P. Nováček, "Analyses of triaxial accelerometer calibration algorithms," *IEEE Sensors J.*, vol. 12, no. 5, pp. 1157–1165, May 2012.

[30] *Model 900 Biaxial Clinometer*, Data Sheet, Appl. Geomechanics, Santa Cruz, CA, USA, 1995.

[31] *Low-Cost 2g Dual Axis Accelerometer With Digital Output, ADXL 202E*. Analog Devices, Inc., Norwood, MA, USA, 2000. [Online]. Available: http://www.analog.com/media/en/technical-documentation/data-sheets/ADXL202E.pdf

[32] *Single-/Dual-Axis iMEMS Accelerometer, ADXL103/ ADXL203*. Analog Devices, Norwood, MA, USA, 2004. [Online]. Available: https://www.analog.com/media/en/technicaldocumentation/data-sheets/adxl103_203.pdf

[33] S. Bütefisch, A. Schoft, and S. Büttgenbach, "Three-axes monolithic silicon low-g accelerometer," *J. Microelectromech. Syst.*, vol. 9, no. 4, pp. 551–556, Dec. 2000.

[34] W. T. Latt, K. C. Veluvolu, and W. T. Ang, "Drift-free position estimation of periodic or quasi-periodic motion using inertial sensors," *Sensors*, vol. 11, no. 6, pp. 5931–5951, May 2011.

[35] W. T. Ang, P. K. Khosla, and C. N. Riviere, "Nonlinear regression model of a low-*G* MEMS accelerometer," *IEEE Sensors J.*, vol. 7, no. 1, pp. 81–88, Jan. 2007.

[36] S. Łuczak, "Dual-axis test rig for mems tilt sensors," *Metrol. Meas. Syst.*, vol. 21, no. 2, pp. 351–362, Jun. 2014.

[37] S.-S. Yun *et al.*, "Fabrication of morphological defect-free vertical electrodes using a (1 1 0) silicon-on-patterned-insulator process for micromachined capacitive inclinometers," *J. Micromech. Microeng.*, vol. 19, no. 3, Mar. 2009, Art. no. 035025.

[38] C. Acar and A. M. Shkel, "Experimental evaluation and comparative analysis of commercial variable-capacitance MEMS accelerometers," *J. Micromech. Microeng.*, vol. 13, no. 5, pp. 634–645, Sep. 2003.

[39] M. Bodnicki and S. Łuczak, "Comments on delay compensation of tilt sensors based on MEMS accelerometer using data fusion Technique," *IEEE Sensors J.*, vol. 18, no. 3, pp. 1333–1335, Feb. 2018.

[40] S. Łuczak, "Fast alignment procedure for MEMS accelerometers," in *Advanced Mechatronics Solutions*, R. Jabłoński and T. Brezina, Eds. Cham, Switzerland: Springer, 2016, pp. 481–487.

[41] S. Łuczak, "Experimental determination of selected parameters of MEMS accelerometers–methodology of experimental studies," *Meas. Autom. Monitor.*, vol. 57, no. 11, pp. 1321–1324, 2011.

[42] S. Łuczak, "Experimental studies of hysteresis in MEMS accelerometers: A commentary," *IEEE Sensors J.*, vol. 15, no. 6, pp. 3492–3499, Jun. 2015.

[43] *Guide to the Expression of Uncertainty in Measurement*, Central Office of Measures, Warsaw, Poland, 1999.

[44] *Expression of the Uncertainty of Measurement in Calibration*, European Co-operation for Acreditation, Amsterdam, The Netherlands, 1999.

[45] S. Łuczak, "Tilt measurements in BMW motorcycles," in *Recent Global Res. Education: Technological Challenges*, R. Jabłoński and R. Szewczyk, Eds. Cham, Switzerland: Springer, 2017, pp. 287–293.

[46] S. Łuczak, M. Zams, and K. Bagiński, "Selected aging effects in triaxial MEMS accelerometers," *J. Sensors*, vol. 2019, pp. 1–11, Nov. 2019.

[47] Z. F. Syed, P. Aggarwal, C. Goodall, X. Niu, and N. El-Sheimy, "A new multi-position calibration method for MEMS inertial navigation systems," *Meas. Sci. Technol.*, vol. 18, no. 7, pp. 1897–1907, Jul. 2007.

[48] S. Łuczak, "Erratum to: Guidelines for tilt measurements realized with MEMS accelerometers," *Int. J. Precis. Eng. Manuf.*, vol. 15, no. 9, pp. 2012–2019, Sep. 2014.

[49] S. Łuczak and W. Oleksiuk, "Increasing accuracy of tilt measurements," *Eng. Mech.*, vol. 14, no. 3, pp. 143–154, 2007.

[50] S. Łuczak, "Effects of misalignments of MEMS accelerometers in tilt measurements," in *Recent Technological and Scientific Advances*, T. Brezina and R. Jabłoński, Eds. Cham, Switzerland: Springer, 2014, pp. 393–400.

Sergiusz Łuczak received the M.S. degree in fine mechanics and the Ph.D. and D.Sc. degrees in mechatronics from the Faculty of Mechatronics, Warsaw University of Technology, Warsaw, Poland, in 1997, 2003, and 2016, respectively.

He is currently an Associate Professor and the Head of the Division of Design of Precision Devices, Institute of Micromechanics and Photonics, Faculty of Mechatronics, Warsaw University of Technology. He has authored more than 50 scientific publications, more than ten inventions, and holds six patents pending. His research has been related to design of mechatronic systems, fine mechanics, and microsystem technology, in particular, experimental studies of tilt sensors and micromachined accelerometers. He has been an Associate Board Member of the journal *Micro and Nanosystems*, and the referee for 13 JCR journals.

Jakub Wierciak received the M.S. degree in fine mechanics and the Ph.D. degree in machine design and maintenance from the Faculty of Mechatronics, Warsaw University of Technology, Warsaw, Poland, in 1981 and 1995, respectively.

He is currently an Assistant Professor with the Division of Design of Precision Devices, Institute of Micromechanics and Photonics, Faculty of Mechatronics, Warsaw University of Technology. He has authored or coauthored more than 100 scientific publications and six patents. His research has been related to the design of mechatronic systems and modeling of electromechanical actuators.

Wojciech Credo received the B.S. and M.S. degrees in mechatronics from the Faculty of Mechatronics, Warsaw University of Technology, Warsaw, Poland, in 2011 and 2013, respectively. He is currently pursuing the Ph.D. degree in mechatronics with the Division of Design of Precision Devices, Institute of Micromechanics and Photonics, Faculty of Mechatronics, Warsaw University of Technology. He is currently an Assistant with the Division of Design of Precision Devices, Institute of Micromechanics and Photonics, Faculty of Mechatronics. He has authored 13 scientific publications and holds one patent pending. His research has been related to design of mechatronic systems, fine mechanics, and the selection of drive systems, in particular, the experimental studies of variable power drive systems.